
LEAVE-GROUP-OUT CROSS-VALIDATION FOR LATENT GAUSSIAN MODELS

Zhedong Liu

Statistics Program, Computer, Electrical and Mathematical Sciences and Engineering Division
King Abdullah University of Science and Technology (KAUST)
Kingdom of Saudi Arabia, Thuwal 23955-6900
zhedong.liu@kaust.edu.sa

Håvard Rue

Statistics Program, Computer, Electrical and Mathematical Sciences and Engineering Division
King Abdullah University of Science and Technology (KAUST)
Kingdom of Saudi Arabia, Thuwal 23955-6900
haavard.rue@kaust.edu.sa

April 10, 2023

ABSTRACT

Evaluating predictive performance is essential after fitting a model and leave-one-out cross-validation is a standard method. However, it is often not informative for a structured model with many possible prediction tasks. As a solution, leave-group-out cross-validation is an extension where the left-out-groups adapt to different prediction tasks. In this paper, we propose an automatic group construction procedure for leave-group-out cross-validation to estimate the predictive performance when the prediction task is not specified. We also propose an efficient approximation of leave-group-out cross-validation for latent Gaussian models. We implement both procedures in the R-INLA software.

Keywords: Cross-Validation, Structured Models, Latent Gaussian Models, R-INLA

1 Introduction

Predictive performance estimation is an essential task for model assessment. Cross-validation (CV) is a common method to estimate the predictive performance by splitting observed data into a training set and a testing set multiple times [1, 2]. K -fold cross-validation (KCV) is a common form of CV. It randomly divides the data into K folds, and uses one fold to test the performance of the model fitted on the remaining $(K - 1)$ folds. The drawback of this approach is that it estimates the performance of the model trained on a training set whose size is much smaller than the full data set. To make the size of the training set closer to the full data set, we can use leave-one-out cross-validation (LOOCV). LOOCV is a limiting form of KCV, which sequentially takes each data point as a testing set (testing point) to test the performance of the model trained on the remaining $(n - 1)$ data points, where n is the size of the observed data. The usage of KCV is mainly out of the purpose of reducing computational burden, thus we view KCV as an alternative of LOOCV when LOOCV is unavailable.

The intuition behind CV is using training sets to represent the observed data set and using testing sets to represent the unobserved data, which is expressed formally in [3]. A proper CV strategy has a relationship between training sets and testing sets similar to the relationship between observed data and unobserved data, and the definition of the unobserved data is determined by the prediction task. Therefore, we should ideally make our CV strategies mimic desired prediction tasks. Unfortunately, this is not common practice. The purpose of this paper is to improve the current practice.

LOOCV and KCV are designed for unstructured models, which assume data are sampled independently from an identical distribution. In this scenario, the prediction task is often defined by predicting a new data point sampled

from the same distribution as the observed data. However, in structured models, where the data are not independently sampled from an identical distribution, multiple prediction tasks exist. For instance, in time series, the prediction could be predicting the response in an independent replicate of the observed time series, forecasting the response in the future of the observed time series, or interpolating a missing value in the observed time series. LOOCV in time series mimics the interpolation task, which is seldom considered a prediction task, and the meaning of KCV in times series, also in general structured models, can not be defined clearly if we only run KCV once because each fold in KCV implies different predictions.

LOOCV is generally over-optimistic about the predictive performance when a model is structured and the task is not interpolation, which is an issue discussed extensively in [4]. The focus of this paper is on structured models and modifying LOOCV to accommodate these types of models.

The deficiency of naively employing LOOCV has also been noticed by many researchers in practice. Here we highlight some specific studies in the literature.

- In a biomedical study [5], a multi-level model is used for diagnosis. Their data are collected from different subjects, and each subject has some records. Researchers recommend the subject-wise CV when the model is used for a diagnosis of newly recruited subjects. The subject-wise CV uses all the records not from a specific subject to train the model and uses the records from the subject to validate the prediction. LOOCV or record-wise CV is expected to be too optimistic since the information from the same subject is used for prediction.
- In a study from the petroleum industry [6], a time series model is used for forecasting. Researchers use leave-future-out cross-validation (LFOCV) [7] to evaluate the model’s ability to forecast the production of tight oil wells. LFOCV uses the observations that happen before a time point to train a model and exploits the observation at that time point to evaluate the predictive performance. LOOCV will produce an overly optimistic result since we infer the testing points using their future but we can only use the history to forecast future data.
- In a paleogeology study [8], spatial models are used for predicting species assemblages and environmental conditions in an area geographically separated from the observed area. Researchers use h-block cross-validation (HCV) [9] to estimate the models’ predictive performance. In HCV, along with the testing point, observations within h km of it are omitted from the training set. LOOCV is again not appropriate due to its usage of unavailable information.

CV variants in the studies adapt to different prediction tasks by adjusting the training sets for each testing set. We can also make LOOCV adapt to the prediction tasks by changing the training set for each data point. We call the adapted LOOCV leave-group-out cross-validation (LGOCV) since the adaptations are done by leaving a group of data out from the training sets. The groups are defined manually to make the prediction task implicitly implied by CV more similar to the desired prediction task.

In some modeling scenarios, we may not have a primary prediction task, but we still want to have an easy-to-use quantity to describe the predictive performance. We can roughly classify prediction tasks into two types, interpolation tasks and extrapolation tasks. In extrapolation tasks, the observed data provide less information to predict the new data. The meaning of the interpolation and the extrapolation varies in different models. Interpolation tasks are exemplified by padding missing values in time series [10, 11] and kriging in geostatistics [12]. Extrapolation tasks are represented by forecasting in a time series model, predicting data on a territory far away from the observations’ location in a spatial model, or predicting data measured from an unobserved stratum in a multilevel model. LOOCV often implies an interpolation task, while an extrapolation task is often considered as prediction in structured models.

In this paper, we also propose an automatic group construction method for latent Gaussian models (LGMs) [13, 14] to better assist modelers to assess their models when the manual groups are not available. The automatically constructed group consists of data points most dependent on the testing point, therefore the testing point will be less dependent on the resulting training set. The aim of our automatic LGOCV is to propose a better default criterion than LOOCV for structured models. If a clear prediction task exists, we recommend using LGOCV designed for the prediction task. Otherwise, the proposed automatized LGOCV is a better option because it reveals more extrapolation performance than LOOCV.

The brute-force way to compute CV is straightforward as we only need to fit models on all possible training sets and compute the utility on the corresponding testing set. However, the computational cost of the brute-force way is prohibitive because a single fit of a modern statistical model is costly. Thus several methods are proposed to compute CV efficiently for different models: [13] approximates LOOCV by correcting the approximated posterior marginal distributions; [15] computes LOOCV using Pareto-smoothed importance sampling (PIS); [16] computes the closed form of leave-one-out prediction errors and variance for kriging in Gaussian process; [17] extends the results in [16]

to compute KCV prediction errors and variance. For Gaussian linear regression, closed-form solutions of LOOCV are well-known. Also, many methods were proposed to compute variants of CV for some structured models by approximation [7, 18, 3].

In this paper, we make LGOCV computationally feasible by deriving an efficient and accurate approximation of LGOCV for LGMs. The automatic group construction procedure and the approximation of LGOCV given groups are implemented in the R-INLA software[13].

The plan for the paper is as follows. Section 2 contains preliminaries on Bayesian cross-validation and LGMs. Section 3 explains the automatic group construction. Section 4 discusses the reason we prefer leave-group-out cross-validation in structured models. Section 5 discusses the approximation of LGOCV. Section 6 compares the approximated LGOCV with the exact LGOCV computed by Markov chain Monte Carlo (MCMC) and demonstrates its use in some real data applications. We end with a general discussion in Section 7.

2 Preliminaries

2.1 Bayesian Cross-Validation

In the Bayesian framework, if we fit a model on a data set \mathbf{y} , we will obtain a posterior distribution $\pi(\phi|\mathbf{y})$, where ϕ are the model parameters. Bayesian prediction relies on a predictive distribution

$$\pi(\tilde{Y}|\mathbf{y}) = \int \pi(\tilde{Y}|\phi, \mathbf{y})\pi(\phi|\mathbf{y})d\phi \quad (1)$$

where \tilde{Y} is an unobserved data point, and the form of $\pi(\tilde{Y}|\phi, \mathbf{y})$ is determined by the prediction task. $\pi(\tilde{Y}|\mathbf{y})$ is validated by external knowledge on \tilde{Y} , for example, a hypothetical generating process of \tilde{Y} or actually observed \tilde{Y} . If a future observation, \tilde{y} , is observed, $\pi(\tilde{Y}|\mathbf{y})$ can be validated against \tilde{y} using a utility function or a loss function. A typical utility function is $u(\tilde{y}, \mathbf{y}) = \log \pi(\tilde{Y} = \tilde{y}|\mathbf{y})$.

The idea of LOOCV is using the pair (y_i, \mathbf{y}_{-i}) as a surrogate of (\tilde{y}, \mathbf{y}) , where y_i is the testing point, and \mathbf{y}_{-i} is the training set. To make the testing point and the training set a better proxy of the new data and the observed data, leave-group-out cross-validation (LGOCV) uses the pair (y_i, \mathbf{y}_{-I_i}) as a surrogate of (\tilde{y}, \mathbf{y}) instead, where I_i is an index set containing indices of data removed from the training set. The purpose of I_i is to make (\tilde{y}, \mathbf{y}) and (y_i, \mathbf{y}_{-I_i}) more similar given a prediction task.

With LGOCV, the mean log predictive density is

$$U_{\text{LGOCV}} = \frac{1}{n} \sum_{i=1}^n \log \pi(Y_i = y_i|\mathbf{y}_{-I_i}), \quad (2)$$

and the mean square error is

$$L_{\text{LGOCV}} = \frac{1}{n} \sum_{i=1}^n (E[Y_i|\mathbf{y}_{-I_i}] - y_i)^2. \quad (3)$$

We can also use different aggregation methods and utility (loss) functions [19, 20] to validate predictions. I_i can be modified to make LGOCV identical to many variants of CV, including subject-wise CV in [5], LFOCV in [6, 7], HCV in [8, 9], and LOOCV.

2.2 Latent Gaussian Models

In this section, we briefly introduce Latent Gaussian Models and its inference using integrated nested Laplace approximation (INLA) [13, 21, 14, 22] to help the readers follow the coming sections. The LGMs can be formulated by

$$\begin{aligned} y_i|\eta_i, \boldsymbol{\theta} &\sim \pi(y_i|\eta_i, \boldsymbol{\theta}), \\ \boldsymbol{\eta} &= \mathbf{A}\mathbf{f}, \\ \mathbf{f}|\boldsymbol{\theta} &\sim N(0, \mathbf{P}_{\mathbf{f}}(\boldsymbol{\theta})), \\ \boldsymbol{\theta} &\sim \pi(\boldsymbol{\theta}). \end{aligned} \quad (4)$$

In LGMs, each y_i is independent conditioning on its corresponding linear predictor η_i and hyperparameters $\boldsymbol{\theta}$; $\boldsymbol{\eta}$ is a linear combination of \mathbf{f} , which is assigned with a Gaussian prior with zero mean and a precision matrix parameterized by $\boldsymbol{\theta}$; \mathbf{A} is the design matrix mapping \mathbf{f} to $\boldsymbol{\eta}$; $\pi(\boldsymbol{\theta})$ is a prior density of hyperparameters.

The model is quite general because \mathbf{f} can be a combination of many modeling components, including linear model, spatial components, temporal components, spline components, etc. It is also common with linear constraints on the latent effects \mathbf{f} [23].

We can approximate $\pi(\mathbf{f}|\boldsymbol{\theta}, \mathbf{y})$ and $\pi(\boldsymbol{\theta}|\mathbf{y})$ at some configurations, $\boldsymbol{\theta}_1 \dots \boldsymbol{\theta}_k$, using INLA. The configurations are located around the mode of $\pi(\boldsymbol{\theta}|\mathbf{y})$, denoted by $\boldsymbol{\theta}^*$, for numerical integration. Approximations of $\pi(\boldsymbol{\eta}|\boldsymbol{\theta}, \mathbf{y})$ are computed using the linear relation, $\boldsymbol{\eta} = \mathbf{A}\mathbf{f}$. The Gaussian approximation of $\pi(\mathbf{f}|\boldsymbol{\theta}, \mathbf{y})$ plays an essential role, which is outlined as follows.

We have $\pi(\mathbf{f}|\boldsymbol{\theta}, \mathbf{y})$ for a given $\boldsymbol{\theta}$,

$$\pi(\mathbf{f}|\boldsymbol{\theta}, \mathbf{y}) \propto \exp \left\{ -\frac{1}{2} \mathbf{f}^T \mathbf{P}_f(\boldsymbol{\theta}) \mathbf{f} + \sum_{i=1}^n \log(\pi(y_i|\eta_i, \boldsymbol{\theta})) \right\}, \quad (5)$$

whose mode is $\boldsymbol{\mu}_f(\boldsymbol{\theta}, \mathbf{y})$. The Gaussian approximation of $\pi(\mathbf{f}|\boldsymbol{\theta}, \mathbf{y})$ is

$$\pi_G(\mathbf{f}|\boldsymbol{\theta}, \mathbf{y}) \propto \exp \left\{ -\frac{1}{2} \mathbf{f}^T (\mathbf{P}_f(\boldsymbol{\theta}) + \mathbf{A}^T \mathbf{C}(\boldsymbol{\theta}, \mathbf{y}) \mathbf{A}) \mathbf{f} + \mathbf{A}^T \mathbf{b}(\boldsymbol{\theta}, \mathbf{y}) \mathbf{f} \right\}. \quad (6)$$

In (6), $b_i(\boldsymbol{\theta}, \mathbf{y}) = g'_i(\eta_i^*) - g''_i(\eta_i^*)\eta_i^*$, and \mathbf{C} is a diagonal matrix with $C_{ii}(\boldsymbol{\theta}, \mathbf{y}) = -g''_i(\eta_i^*)$, where $g_i(\eta_i) = \log(\pi(y_i|\eta_i, \boldsymbol{\theta}))$ and $\eta_i^* = \mathbf{A}_i \boldsymbol{\mu}_f(\boldsymbol{\theta}, \mathbf{y})$ with \mathbf{A}_i being i th row of \mathbf{A} . The Gaussian approximation is denoted by,

$$\mathbf{f}|\boldsymbol{\theta}, \mathbf{y} \sim N(\boldsymbol{\mu}_f(\boldsymbol{\theta}, \mathbf{y}), \mathbf{Q}_f(\boldsymbol{\theta}, \mathbf{y})), \quad (7)$$

where $\boldsymbol{\mu}_f(\boldsymbol{\theta}, \mathbf{y}) = \mathbf{Q}_f(\boldsymbol{\theta}, \mathbf{y})^{-1} \mathbf{A}^T \mathbf{b}(\boldsymbol{\theta}, \mathbf{y})$ and $\mathbf{Q}_f(\boldsymbol{\theta}, \mathbf{y}) = \mathbf{P}_f(\boldsymbol{\theta}) + \mathbf{A}^T \mathbf{C}(\boldsymbol{\theta}, \mathbf{y}) \mathbf{A}$ are the approximated posterior mean and precision matrix of \mathbf{f} given $\boldsymbol{\theta}$. The mean of Gaussian approximation, $\boldsymbol{\mu}_f(\boldsymbol{\theta}, \mathbf{y})$, can be further improved using low rank variational Bayes using method in [22].

3 Automatic Group Construction

The intention of our automatic construction is to make the testing points less dependent on the corresponding training sets such that the LGOCV mimics an extrapolation task, in which the unobserved data is often assumed less dependent on the observed data.

In LGMs, the dependency of data is specified by the dependency of linear predictors in (4). The linear predictors are designed to have a Gaussian prior and approximated to be Gaussian in posterior given $\boldsymbol{\theta}$, therefore we can use the correlation matrix of $\boldsymbol{\eta}$ to represent dependency. For fixed $\boldsymbol{\theta}$, we have correlation matrices derived from $\mathbf{P}_f(\boldsymbol{\theta})$ and $\mathbf{Q}_f(\boldsymbol{\theta}, \mathbf{y})$. We call the former one prior correlation matrix, denoted by $\mathbf{R}_{prior}(\boldsymbol{\theta})$ and the later one posterior correlation matrix, denoted by $\mathbf{R}_{post}(\boldsymbol{\theta})$. We evaluate those correlation matrices at $\boldsymbol{\theta}^*$. Note that the correlation matrices are rarely fully evaluated and stored in order to avoid computational burden as they are dense and large. We will use either $\mathbf{R}_{post} = \mathbf{R}_{post}(\boldsymbol{\theta}^*)$ or $\mathbf{R}_{prior} = \mathbf{R}_{prior}(\boldsymbol{\theta}^*)$ to construct the groups. The correlation matrix for the linear predictors is central in our proposal for the definition of the groups we discuss the implications from each case.

The manually constructed groups are often based on prior knowledge and some interesting effects of \mathbf{f} . To imitate this process, we can compute the correlation matrix from a submatrix of $\mathbf{P}_f(\boldsymbol{\theta})$. The submatrix contains those interesting effects of \mathbf{f} . The correlation matrix, \mathbf{R}_{prior} , derived from the submatrix of the precision matrix is a conditional correlation matrix conditioning on those unselected effects. When we are unknowledgeable about our models, we recommend using \mathbf{R}_{post} to construct groups because data can help us determine the importance of each component.

With a correlation matrix \mathbf{R} , it is natural to choose I_i by including a fixed number of points that are most correlated to η_i into the group. This approach is problematic because many linear predictors are frequently identically correlated to η_i . It is more reasonable to include all the points identically correlated to η_i into I_i if one of them is included. We can define a level set to be all the points with the same absolute correlation to η_i . Then the size of the group is chosen based on the number of level sets, m , considered. The training set and the testing point will be less dependent if we set higher m . In general, we recommend a small number of level sets when \mathbf{R}_{post} is used, like $m = 3$, since the group size will be too large if m is chosen to be high. As an example, in the last application of Section 6, $m = 3$ creates a group with size of 20.

The automatic group construction process is summarized as follows. We set up the construction by choosing the number of the level sets, m , and which correlation matrix to use. Then, for each i , we can have m level sets associated with m largest absolute correlation to η_i . Finally, the union of those level sets is I_i .

We use some examples to demonstrate the group construction process using \mathbf{R}_{prior} . We will see that the automatically constructed groups are similar to the manually constructed groups and many level sets contain multiple members. The

group construction process using R_{post} is the same as using R_{prior} but the resulting groups are affected by \mathbf{y} . We will show the groups constructed by R_{post} in Section 6.

Example (Nested multilevel model). Assume we record students' grades \mathbf{y} and their self-rating \mathbf{x} . A student is from a class; A class is in a school; A school is in a region. We could model this data by an LGM,

$$\begin{aligned}\eta_i &= \mu + c_{j_c(i)} + s_{j_s(i)} + r_{j_r(i)} + \beta x_i, \\ \mathbf{c}, \mathbf{s}, \mathbf{r}, \beta, \mu | \boldsymbol{\theta} &\sim N(0, \mathbf{P}_f(\boldsymbol{\theta})).\end{aligned}\quad (8)$$

In model (8), $j_c(i)$, $j_s(i)$ and $j_r(i)$ map i to student i 's class, school, and region index. $\mathbf{P}_f(\boldsymbol{\theta})$ is a diagonal matrix with $\boldsymbol{\theta} = \{\tau_r, \tau_s, \tau_c, \tau_\beta, \tau_\mu\}$ and $\mathbf{P}_f(\boldsymbol{\theta}) = \text{diag}(\tau_r, \tau_r, \tau_s, \tau_s, \tau_s, \tau_s, \tau_c, \tau_c, \tau_c, \tau_c, \tau_c, \tau_c, \tau_c, \tau_c, \tau_\beta, \tau_\mu)$ which corresponds 2 regions, 2 schools in each region, and 2 classes in each school. For example, in Figure 1, $j_c(12) = 6$, $j_s(12) = 3$, $j_r(12) = 2$.

For simplicity of notation, we assume $\boldsymbol{\theta}^* = \{1, 1, 1, 1, 1\}$. Then the unconditional correlation for η_i and η_j and the correlation conditioning on μ and β are

$$\begin{aligned}\text{corr}(\eta_i, \eta_j) &= \frac{\mathbb{1}_{j_c(i)=j_c(j)} + \mathbb{1}_{j_s(i)=j_s(j)} + \mathbb{1}_{j_r(i)=j_r(j)} + 1 + x_i x_j}{\sqrt{(4 + x_i^2)(4 + x_j^2)}}, \\ \text{corr}(\eta_i, \eta_j | \mu, \beta) &= \frac{\mathbb{1}_{j_c(i)=j_c(j)} + \mathbb{1}_{j_s(i)=j_s(j)} + \mathbb{1}_{j_r(i)=j_r(j)}}{3},\end{aligned}$$

where $\mathbb{1}_A$ is 1 if A is true and 0 otherwise. With the unconditional correlation, the groups reflect the correlation due to x_i and x_j . In practice, the groups may not be desirable because we usually assume \mathbf{x} are sampled randomly without structure.

With the conditional correlation, we have four level sets for each i which associate with absolute correlation equal to $0, \frac{1}{3}, \frac{2}{3}$ and 1. I_i includes all students from the i th student's class when $m = 1$; I_i includes all students from the i th student's school when $m = 2$; I_i includes all students from the i th student's region when $m = 3$; I_i includes all the data when $m = 4$. Groups produced by each number of level sets have a good interpretation in the example. For $m = 1$, the implied prediction task is predicting a student's grade in an unobserved class of an observed school; for $m = 2$, it is predicting a student's grade in an unobserved school of an observed region; for $m = 3$, it is predicting a student's grade in an unobserved region; for $m = 4$, we exclude all the data, which is a prior prediction; the implied prediction task of LOOCV is predicting a student's grade from an observed class. An automatically constructed group using $\text{corr}(\eta_i, \eta_j | \mu, \beta)$ is shown in Figure 1 for $i = 12$ with $m = 2$, which is $I_{12} = \{12, 13, 14, 15, 10, 11\}$.

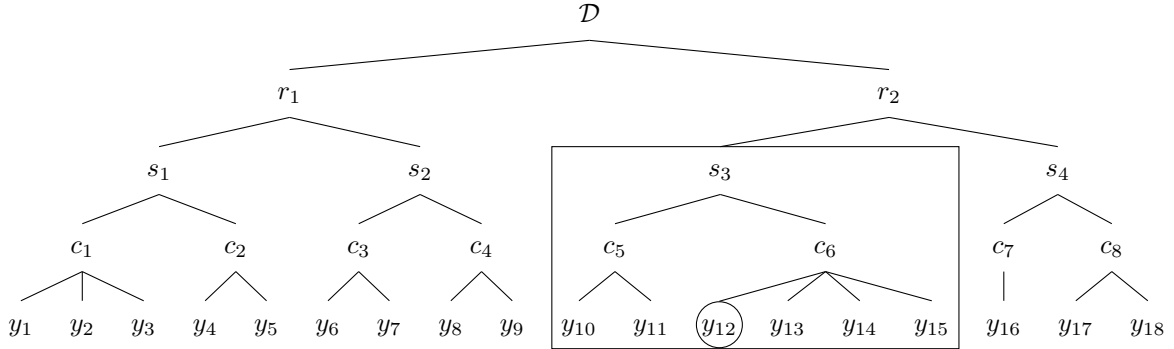


Figure 1: An automatically constructed group for nested multilevel model

We can also get reasonable groups through the spatial correlation when we have a spatial effect in the model.

Example (Spatial Model). Assume each data point is recorded with a spatial location s_i . The latent linear predictor can be specified by

$$\eta_i = \mu + f_{s_i}.$$

f_s is often modeled by a Gaussian field with zero mean and an isotropic spatial correlation. Using the correlation derived from the spatial effects, I_i includes data within a circle centered by the testing point with a radius determined by m . By choosing m such that $\text{var}(\eta_i | \boldsymbol{\eta}_{-I}) \approx \text{var}(\eta_i)$, the implied prediction task is predicting a data point from a remote area or a data point from a replicate of the Gaussian process. Figure 2 shows an automatically constructed group with $m = 5$ with the solid point as the testing point. In the figure, the data in the circle are the group to be removed from the training set, and the group size is 6.

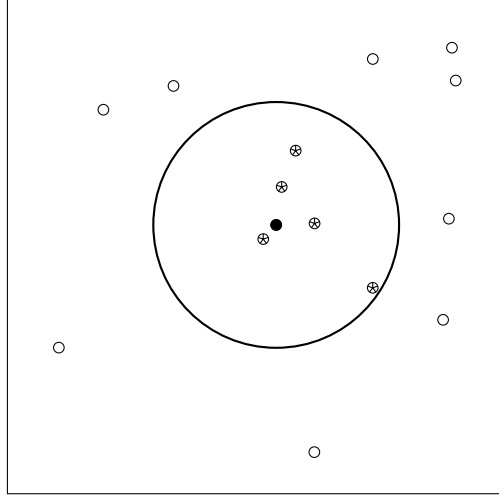


Figure 2: An automatically constructed group for a spatial model

In the examples, the interesting model components for group construction are clear. However, in practice, we can encounter models with multiple important model components in the sense that they could be potentially included for group construction, like the last example in section 6. In this case, we recommend using R_{post} with small m if we can not decide which components are more important.

4 A Discussion on Leave-one-out Cross-Validation and Leave-group-out Cross-Validation

The discussion in this section assumes the existence of an underlying true model that is responsible for both observed and future data. However, it is common that the true model is either inaccessible or non-existent in practical applications. Here we assume the observed data, \mathbf{Y} , and the unobserved data, $\tilde{\mathbf{Y}}$ sampled from a true model with $\pi_T(\mathbf{Y}, \tilde{\mathbf{Y}})$ as its probability density, where the density can be decomposed into the form:

$$\pi_T(\mathbf{Y}, \tilde{\mathbf{Y}}) = \pi_T(\tilde{\mathbf{Y}}|\mathbf{Y})\pi_T(\mathbf{Y}).$$

The objective of utilizing CV is to validate the predictions made by equation (1). The quality of the prediction can be assessed using a logarithmic utility function, which is expressed as follows:

$$G(\mathbf{Y}) = E[\log \pi(\tilde{\mathbf{Y}}|\mathbf{Y})]. \quad (9)$$

In (9), $E[\cdot]$ represents the expectation taken over $\tilde{\mathbf{Y}}$, with probability density $\pi_T(\tilde{\mathbf{Y}}|\mathbf{Y})$.

Assuming that the true model is unstructured, it follows all the marginal distribution are the same. Let the LOOCV utility be $U_{\text{LOOCV}}(\mathbf{Y}) = \frac{1}{n} \sum_{i=1}^n \log \pi(Y_i|\mathbf{Y}_{-i})$. In this scenario, according to [24, 25], the expected utility of the logarithmic utility function $G(\mathbf{Y})$ can be expressed as follows:

$$E[G(\mathbf{Y})] = E[U_{\text{LOOCV}}(\mathbf{Y})] + o\left(\frac{1}{n}\right), \quad (10)$$

where $E[\cdot]$ denotes the expectation taken over \mathbf{Y} , with probability density function $\pi_T(\mathbf{Y})$, and n is the length of \mathbf{Y} . The empirical convergence of the variance of both $G(\mathbf{Y})$ and $U_{\text{LOOCV}}(\mathbf{Y})$ to zero implies that $U_{\text{LOOCV}}(\mathbf{Y}) \approx G(\mathbf{Y})$ for large n given a realization. Note, this scenario is applicable to regression with response and covariates independently sampled from an identical joint distribution.

In the absence of the assumption of identical and independent distribution of the data, i.e. the true model is structured, various forms of $\pi_T(\tilde{\mathbf{Y}}, \mathbf{Y})$ can be considered. For example, when data is generated in groups, each group having its own group-specific mean and a universal mean shared by all groups, two prediction scenarios can be set - future data generated in observed groups and future data generated in unobserved groups. These two scenarios correspond to two different $\pi_T(\tilde{\mathbf{Y}}|\mathbf{Y})$ and hence two different $G(\mathbf{Y})$. Similarly, when data is generated with a temporal structure, different

$\pi_T(\tilde{Y}|\mathbf{Y})$ can be used to describe unobserved data, including replicates of a data point at a certain time given its history and future, a data point generated in the future given its history, and data points generated by another replicated time series independent of the observed one, among others. The asymptotic schemes in these scenarios are undefined as well. In the group data example, it's important to consider not just the total number of data points, but also the number of groups and the ratio of the number of groups to the number of data points in each group. The conclusion is that the asymptotic behavior of $U_{\text{LOOCV}}(\mathbf{Y})$ is not well-defined due to the infinite possible combinations of different $G(\mathbf{Y})$ and asymptotic schemes. Therefore, the asymptotic behavior must be studied on a case-by-case basis.

Although the asymptotic behavior of $U_{\text{LOOCV}}(\mathbf{Y})$ is not defined, it is still used in structured models due to the belief that the calculation of $U_{\text{LOOCV}}(\mathbf{Y})$ mimics the prediction process. However, LOOCV only mimics interpolation, which typically have a lower variance in $\pi_T(\tilde{Y}|\mathbf{Y})$ where \mathbf{Y} provides more information for predicting \tilde{Y} . If a specific prediction task is defined, then $\pi_T(\tilde{Y}, \mathbf{Y})$ may be specified according to the task. In this case, I_i can be designed for each i to make $\pi_T(Y_i, \mathbf{Y}_{-I_i})$ a proxy of $\pi_T(\tilde{Y}, \mathbf{Y})$. When no prediction task is available, I_i cannot be designed based on the presumed $\pi_T(\tilde{Y}, \mathbf{Y})$, but we still want to evaluate our model beyond interpolation performance. Hence, we suggest constructing I_i such that \mathbf{Y}_{-I_i} provides less information for predicting Y_i . Since $\pi_T(\mathbf{Y})$ is also not available, we use either the posterior or prior correlation of linear predictors from a belief model [26] to gauge the amount of information for predicting Y_i .

In conclusion, if there are specified prediction tasks, U_{LGOCV} with I_i designed according to those tasks should be used to assess the prediction. If no tasks are specified, U_{LGOCV} with automatically generated groups can be used to assess the model's predictive capabilities rather than its interpolation abilities.

5 Approximation of Leave-group-out Cross-Validation

This section discusses how to approximate $\pi(Y_i|\mathbf{y}_{-I_i})$. The results are straightforward but great care is needed to make all the corner cases numerically stable. Empirically, this new approach is more accurate and stable than the one published in [13] when $I_i = i$.

We start by writing $\pi(Y_i|\mathbf{y}_{-I_i})$ as a nested integral,

$$\pi(Y_i|\mathbf{y}_{-I_i}) = \int_{\boldsymbol{\theta}} \pi(Y_i|\boldsymbol{\theta}, \mathbf{y}_{-I_i}) \pi(\boldsymbol{\theta}|\mathbf{y}_{-I_i}) d\boldsymbol{\theta} \quad (11)$$

$$\pi(Y_i|\boldsymbol{\theta}, \mathbf{y}_{-I_i}) = \int \pi(Y_i|\eta_i, \boldsymbol{\theta}) \pi(\eta_i|\boldsymbol{\theta}, \mathbf{y}_{-I_i}) d\eta_i. \quad (12)$$

The integral (11) is computed by the numerical integration [13], and the integral (12) is computed by Gauss-Hermite quadratures [27] as $\pi(\eta_i|\boldsymbol{\theta}, \mathbf{y}_{-I_i})$ will be approximated by a Gaussian distribution. The key to the accuracy of (12) is that the likelihood, $\pi(Y_i|\eta_i, \boldsymbol{\theta})$, is exact such that small approximation errors of $\pi(\eta_i|\boldsymbol{\theta}, \mathbf{y}_{-I_i})$ diminish due to the integration. The accuracy of (11) relies on the accuracy of (12) and the assumption that the removal of \mathbf{y}_{I_i} does not have drastic impact on $\pi(\boldsymbol{\theta}|\mathbf{y})$.

The computation of the nested integrals boils down to the computation of $\pi(\eta_i|\boldsymbol{\theta}, \mathbf{y}_{-I_i})$ and $\pi(\boldsymbol{\theta}|\mathbf{y}_{-I_i})$. We will approximate $\pi(\eta_i|\boldsymbol{\theta}, \mathbf{y}_{-I_i})$ by a Gaussian based on (6), denoted by $\pi_G(\eta_i|\boldsymbol{\theta}, \mathbf{y}_{-I_i})$, and $\pi(\boldsymbol{\theta}|\mathbf{y}_{-I_i})$ by correcting $\pi(\boldsymbol{\theta}|\mathbf{y})$. We further improve the mean of $\pi_G(\eta_i|\boldsymbol{\theta}, \mathbf{y}_{-I_i})$ using variational Bayes [22] in the implementation. In this section, we focus on the explanation of computing $\pi_G(\eta_i|\boldsymbol{\theta}, \mathbf{y}_{-I_i})$ and $\pi(\boldsymbol{\theta}|\mathbf{y}_{-I_i})$.

Compute $\pi_G(\eta_i|\boldsymbol{\theta}, \mathbf{y}_{-I_i})$

The mean and variance of $\pi_G(\eta_i|\boldsymbol{\theta}, \mathbf{y}_{-I_i})$ can be obtained by

$$\begin{aligned} \mu_{\eta_i}(\boldsymbol{\theta}, \mathbf{y}_{-I_i}) &= \mathbf{A}_i \boldsymbol{\mu}_f(\boldsymbol{\theta}, \mathbf{y}_{-I_i}), \\ \sigma_{\eta_i}^2(\boldsymbol{\theta}, \mathbf{y}_{-I_i}) &= \mathbf{A}_i \mathbf{Q}_f^{-1}(\boldsymbol{\theta}, \mathbf{y}_{-I_i}) \mathbf{A}_i^T. \end{aligned} \quad (13)$$

The computation of $\pi_G(\mathbf{f}|\boldsymbol{\theta}, \mathbf{y}_{-I_i})$ requires the mode of $\pi(\mathbf{f}|\boldsymbol{\theta}, \mathbf{y}_{-I_i})$ for each i at each configuration of $\boldsymbol{\theta}$, which is computationally expensive. With (6), we use an approximation to avoid the optimization step,

$$\mathbf{Q}_f(\boldsymbol{\theta}, \mathbf{y}_{-I_i}) \approx \tilde{\mathbf{Q}}_f(\boldsymbol{\theta}, \mathbf{y}_{-I_i}) = \mathbf{Q}_f(\boldsymbol{\theta}, \mathbf{y}) - \mathbf{A}_{I_i}^T \mathbf{C}_{I_i}(\boldsymbol{\theta}, \mathbf{y}) \mathbf{A}_{I_i}, \quad (14)$$

$$\boldsymbol{\mu}_f(\boldsymbol{\theta}, \mathbf{y}_{-I_i}) \approx \tilde{\boldsymbol{\mu}}_f(\boldsymbol{\theta}, \mathbf{y}_{-I_i}) = \tilde{\mathbf{Q}}_f(\boldsymbol{\theta}, \mathbf{y}_{-I_i})^{-1} (\mathbf{A}^T \mathbf{b}(\boldsymbol{\theta}, \mathbf{y}) - \mathbf{A}_{I_i}^T \mathbf{b}_{I_i}(\boldsymbol{\theta}, \mathbf{y})), \quad (15)$$

where \mathbf{A}_{I_i} is a submatrix of \mathbf{A} formed by rows of \mathbf{A} , $\mathbf{b}_{I_i}(\boldsymbol{\theta}, \mathbf{y})$ is a subvector of $\mathbf{b}(\boldsymbol{\theta}, \mathbf{y})$, and $\mathbf{C}_{I_i}(\boldsymbol{\theta}, \mathbf{y})$ is a principal submatrix of $\mathbf{C}(\boldsymbol{\theta}, \mathbf{y})$. (14) and (15) are moments of the Gaussian approximation of $\pi(\mathbf{f}|\boldsymbol{\theta}, \mathbf{y}_{-I_i})$ on the mode of

$\pi(\mathbf{f}|\boldsymbol{\theta}, \mathbf{y})$. Hence, when the posterior is Gaussian, the approximation is exact. It seems easy to obtain the moments using (13), but the decomposition of $\tilde{\mathbf{Q}}_{\mathbf{f}}(\boldsymbol{\theta}, \mathbf{y}_{-I_i})$ is too expensive. To avoid the decomposition of $\tilde{\mathbf{Q}}_{\mathbf{f}}(\boldsymbol{\theta}, \mathbf{y}_{-I_i})$, we use the linear relation $\boldsymbol{\eta}_{I_i} = \mathbf{A}_{I_i}\mathbf{f}$ to map all the computation on \mathbf{f} to $\boldsymbol{\eta}_{I_i}$. We compute $\boldsymbol{\Sigma}_{\boldsymbol{\eta}_{I_i}}(\boldsymbol{\theta}, \mathbf{y}_{-I_i})$ and $\boldsymbol{\mu}_{\boldsymbol{\eta}_{I_i}}(\boldsymbol{\theta}, \mathbf{y}_{-I_i})$ through $\boldsymbol{\Sigma}_{\boldsymbol{\eta}_{I_i}}(\boldsymbol{\theta}, \mathbf{y})$ and $\boldsymbol{\mu}_{\boldsymbol{\eta}_{I_i}}(\boldsymbol{\theta}, \mathbf{y})$ as shown in Appendix A with a low rank representation, where $\boldsymbol{\Sigma}_{\boldsymbol{\eta}_{I_i}}(\boldsymbol{\theta}, \mathbf{y})$ is the posterior covariance matrix of $\boldsymbol{\eta}_{I_i}$ and $\boldsymbol{\Sigma}_{\boldsymbol{\eta}_{I_i}}(\boldsymbol{\theta}, \mathbf{y}_{-I_i})$ is the covariance matrix of $\boldsymbol{\eta}_{I_i}$ with \mathbf{y}_{I_i} left out. The computation of $\boldsymbol{\Sigma}_{\boldsymbol{\eta}_{I_i}}(\boldsymbol{\theta}, \mathbf{y})$ is non-trivial especially when linear constraints are applied, which is demonstrated in Appendix B.

The approximation is more accurate when $\pi(\boldsymbol{\eta}_i|\boldsymbol{\theta}, \mathbf{y}_{-I_i})$ is close to Gaussian. The Gaussianity of $\boldsymbol{\eta}_i|\boldsymbol{\theta}, \mathbf{y}_{-I_i}$ comes from three sources. Firstly, $\pi(\boldsymbol{\eta}_i|\boldsymbol{\theta}, \mathbf{y}_{-I_i})$ is asymptotically Gaussian [28], which tends to be applicable when $\boldsymbol{\eta}_i$ is connected to large amount of data. Secondly, $\pi(\boldsymbol{\eta}_i|\boldsymbol{\theta}, \mathbf{y}_{-I_i})$ is dominated by the Gaussian prior, which happens when $\boldsymbol{\eta}_i$ is connected to few data. Thirdly, the likelihood is close to Gaussian.

Approximate $\pi(\boldsymbol{\theta}|\mathbf{y}_{-I_i})$

To approximate $\pi(\boldsymbol{\theta}|\mathbf{y}_{-I_i})$, we consider the relation,

$$\pi(\boldsymbol{\theta}|\mathbf{y}_{-I_i}) \propto \frac{\pi(\boldsymbol{\theta}|\mathbf{y})}{\pi(\mathbf{y}_{I_i}|\boldsymbol{\theta}, \mathbf{y}_{-I_i})},$$

where we can approximate $\pi(\boldsymbol{\theta}|\mathbf{y})$ at some configurations [13]. We need to compute $\pi(\mathbf{y}_{I_i}|\boldsymbol{\theta}, \mathbf{y}_{-I_i})$, which is

$$\pi(\mathbf{y}_{I_i}|\boldsymbol{\theta}, \mathbf{y}_{-I_i}) \approx \int \pi(\mathbf{y}_{I_i}|\boldsymbol{\eta}_{I_i}, \boldsymbol{\theta})\pi_G(\boldsymbol{\eta}_{I_i}|\boldsymbol{\theta}, \mathbf{y}_{-I_i})d\boldsymbol{\eta}_{I_i}.$$

A Laplace approximation approximates this integral,

$$\pi_{LA}(\mathbf{y}_{I_i}|\boldsymbol{\theta}, \mathbf{y}_{-I_i}) = \frac{\pi(\mathbf{y}_{I_i}|\boldsymbol{\eta}_{I_i}^*, \boldsymbol{\theta})\pi_G(\boldsymbol{\eta}_{I_i}^*|\boldsymbol{\theta}, \mathbf{y}_{-I_i})}{\pi_G(\boldsymbol{\eta}_{I_i}^*|\boldsymbol{\theta}, \mathbf{y})}, \quad (16)$$

where $\boldsymbol{\eta}_{I_i}^*$ is the mode of $\pi_G(\boldsymbol{\eta}_{I_i}^*|\boldsymbol{\theta}, \mathbf{y})$. Note that the correction of hyperparameter reuses $\pi_G(\boldsymbol{\eta}_{I_i}|\boldsymbol{\theta}, \mathbf{y}_{-I_i})$ and $\pi_G(\boldsymbol{\eta}_{I_i}|\boldsymbol{\theta}, \mathbf{y})$.

Approximate LGOCV Mean Square Error

With approximations of $\pi(\boldsymbol{\theta}|\mathbf{y}_{-I_i})$ and $\pi(\boldsymbol{\eta}_i|\boldsymbol{\theta}, \mathbf{y}_{-I_i})$, the computation of (2) is done. One can also compute the leave-group-out version of mean square loss as shown in (3). The expectation of the response is a simple integral,

$$E[Y_i|\mathbf{y}_{-I_i}] = \int_{\boldsymbol{\theta}} \int_{\boldsymbol{\eta}_i} E[Y_i|\boldsymbol{\eta}_i, \boldsymbol{\theta}]\pi(\boldsymbol{\eta}_i|\boldsymbol{\theta}, \mathbf{y}_{-I_i})\pi(\boldsymbol{\theta}|\mathbf{y}_{-I_i})d\boldsymbol{\eta}_id\boldsymbol{\theta},$$

where the model gives $E[Y_i|\boldsymbol{\eta}_i, \boldsymbol{\theta}]$. Other loss and utility functions can be achieved similarly.

6 Simulations and Applications

This section provides a simulated example and three real data applications. We start with a simulated example to verify the accuracy of the approximation in a multilevel model with different responses. We continue with a time series forecasting simulation to compare the results of LGOCV with automatically constructed groups and LFOCV. Then, we fit a model for disease mapping to compare groups constructed by different strategies. In the end, we apply our method to a model with complex structures on a large data set [29].

Simulated Multilevel Model with Various Responses

This simulated example intends to show the accuracy of the approximation compared with MCMC. We consider a multilevel model [2],

$$\begin{aligned} y_i|\boldsymbol{\eta}_i, \boldsymbol{\theta} &\sim \text{Likelihood}(\boldsymbol{\eta}_i, \boldsymbol{\theta}), \\ \boldsymbol{\eta}_i &= \boldsymbol{\mu} + \mathbf{s}_{j_s(i)}, \\ \mathbf{s}, \boldsymbol{\mu}|\boldsymbol{\theta} &\sim N(0, \mathbf{P}_{\mathbf{f}}(\boldsymbol{\theta})), \end{aligned} \quad (17)$$

which is a model describing observations sampled from different groups. In this model, $\mathbf{P}_{\mathbf{f}}(\boldsymbol{\theta})$ is a diagonal matrix similar to $\mathbf{P}_{\mathbf{f}}(\boldsymbol{\theta})$ in (8). We set the prior precision of the intercept $\tau_{\boldsymbol{\mu}} = 10^{-4}$ and assign a normal prior with mean 0

and precision 10^{-4} to $\log \tau_s$. We will consider three cases where y_i has different likelihoods. For a Gaussian response, the precision of the likelihood is fixed to be 1. For a binomial response, we set the number of trials to be 20 and use a logit link. For an exponential response, we use a log link. There are natural groups in this model, which are used for LGOCV. This is a computationally hard case since the testing point can be only predicted by the intercept after removing the group, which means the removal has a large impact on the posterior.

We simulate data according to the specified model with 10 groups and 10 data points in each group. As a reference, the MCMC runs 10^8 iterations, which makes the Monte Carlo errors negligible. Large size of MCMC samples is required because the predictive distributions are influenced by the tails of $\pi(\eta_i | \boldsymbol{\theta}, \mathbf{y}_{-I_i})$. In Figure 3, (a), (c), and (d) show the data against its group index, which present a clear group structure; (b), (d), and (e) show the comparison of $\pi(Y_i = y_i | \mathbf{y}_{-I_i})$ obtained from the approximations and MCMC. We use Rstan [30] to do MCMC.

This example shows that the approximations are highly accurate. When the response is Gaussian, the approximation almost equals the MCMC results, where the difference is due to MCMC sampling errors while our approach is exact up to numerical integration for this case. Also, under both non-Gaussian cases, the results are close to the long-run MCMC results.

Time Series Forecasting

In this example, we will show that the automatic LGOCV can measure predictive performance of a time series model while LOOCV fails to do so. We fit a time series model on a simulated data set generated according to the model:

$$\begin{aligned} y_i | \eta_i, \boldsymbol{\theta} &\sim N(\eta_i, \tau_y) \\ \eta_i &= \mu + u_i \\ u_i &= \rho u_{i-1} + \epsilon_i \\ \epsilon_i &\sim N(0, \tau_u) \end{aligned}$$

where 2000 data points are simulated, \mathbf{u} is modeled by an AR(1) model, $\rho = 0.9$ is the correlation between two adjacent time point, $\tau_u = 1$ is the precision of the additive noise applied on previous step and $\tau_y = 10$ is the noise applied on the latent field. We fix the hyperparameters to true values in the simulation example. We will estimate $\mu = 2$ and u_i , and the prediction task are t steps forward forecasting for $t = \{1, 2, \dots, 10\}$ using the true model. The natural cross-validation for these prediction tasks is leave-future-out cross-validation (LFOCV) [7]. The group in LFOCV for testing point y_i for t steps forward prediction includes $\mathbf{y}_{(i-t+1):n}$. We can compute LFOCV for every t using utility function (2), which is denoted by $\text{LFOCV}(t)$. To make the training set similar to the data set, the last 500 data points will be used as testing points which means $i = \{1500, \dots, 2000\}$ in (2), and the quantity is averaged over 500 data points. We can also compute LGOCV using automatically constructed groups for number of level sets, $m = \{1, 2, \dots, 10\}$, which is denoted by $\text{LGOCV}(m)$. In this setting, the automatically constructed group for testing point y_i with number of level sets equal to m includes $\mathbf{y}_{\max(0, i-m+1): \min(n, i+m-1)}$. In this model, $\text{LGOCV}(1)$ is equivalent to LOOCV.

To compare LGOCV as a function of m and LFOCV as a function of t , we fit a natural spline to $\text{LFOCV}(t)$. Then, we can map m in the automatic LGOCV to t in LFOCV. In Figure 4, (a) shows the spline fitted on LFOCV, and (b) shows the map from number of level sets to steps ahead. We can see that LOOCV is approximately $\text{LFOCV}(0.4)$, which means LOOCV measures 0.4 steps forward forecasting when the simplest prediction task is one step forward forecasting. $\text{LGOCV}(2)$ is approximately $\text{LFOCV}(1.1)$, which can roughly represent one step forward forecasting performance of the model. As m increases, $\text{LGOCV}(m)$ represents more steps forward forecasting performance. Note that the specific translation between the automatic LGOCV and LFOCV is only valid in this model, which is not for the general setting. In different model, automatic LGOCV has different meaning, and the ambiguity is the cost of being generic.

Disease Mapping

In this example, we will present groups constructed by different automatic group construction strategies on German maps. We will see the differences between those groups, and get an idea to choose a proper group construction strategy. We fit a model for disease mapping based on a data set describing cancer incidence with locations [31, 32, 33]. The data are incidence cases of oral cavity cancer in Germany, 1986-1990 [33]. The response y_i is the number of cases during the five years in area i . The number of cases in region i also depends on the population in that region and their age distribution. The expected number of cases of the disease in region i is calculated based on the age distribution and population such that $\sum_i y_i = \sum_i E_i$, where E_i is the expected counts. The covariate x_i is a measure for tobacco consumption in area i .

We fit the following model on the data set:

$$\begin{aligned} y_i | \eta_i, \boldsymbol{\theta} &\sim \text{Poisson}(E_i \exp(\eta_i)) \\ \eta_i &= \mu + f_{\text{tw}}(x_i) + u_i + v_i, \end{aligned} \tag{18}$$

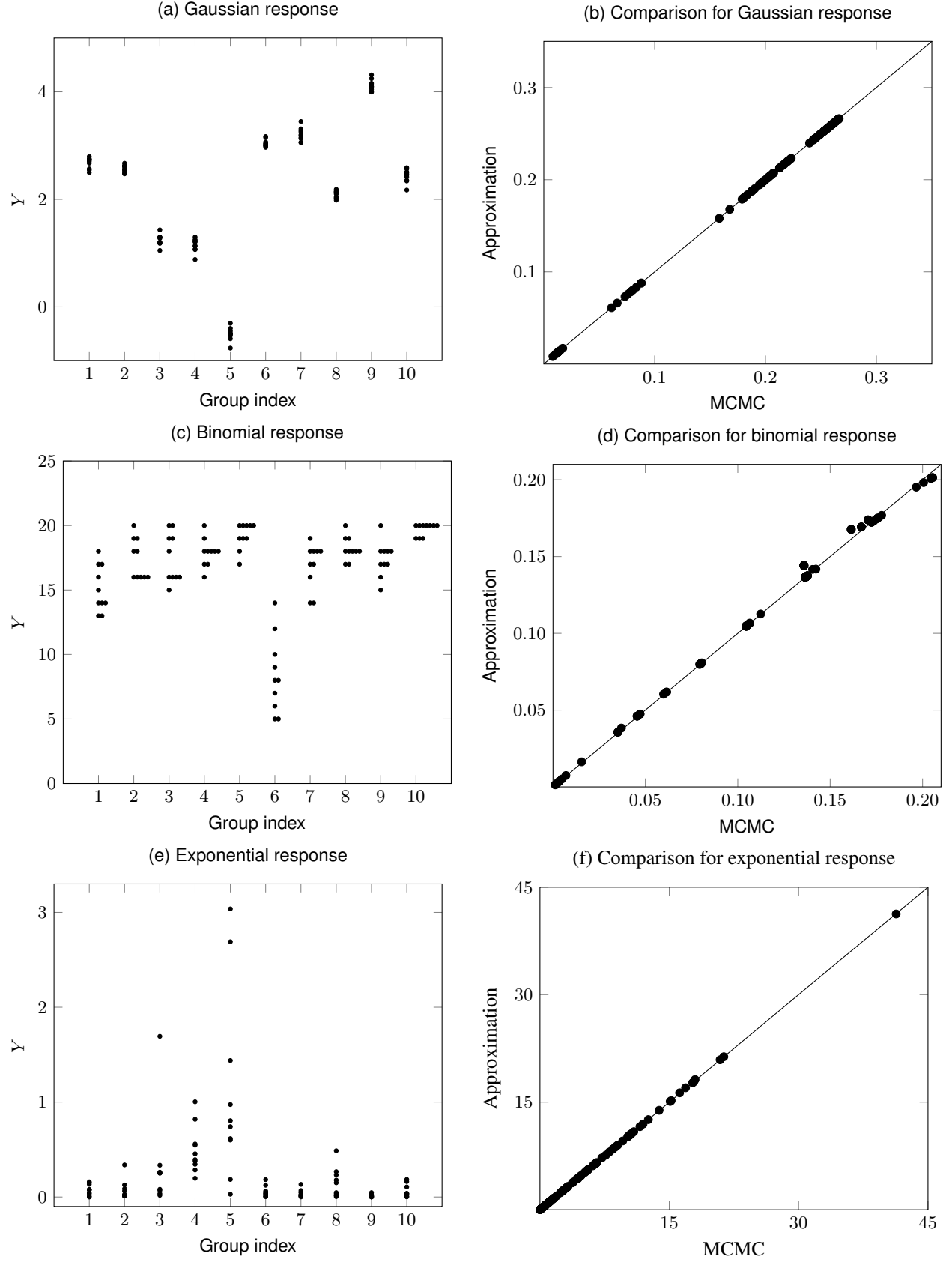


Figure 3: Our approximations compared with MCMC

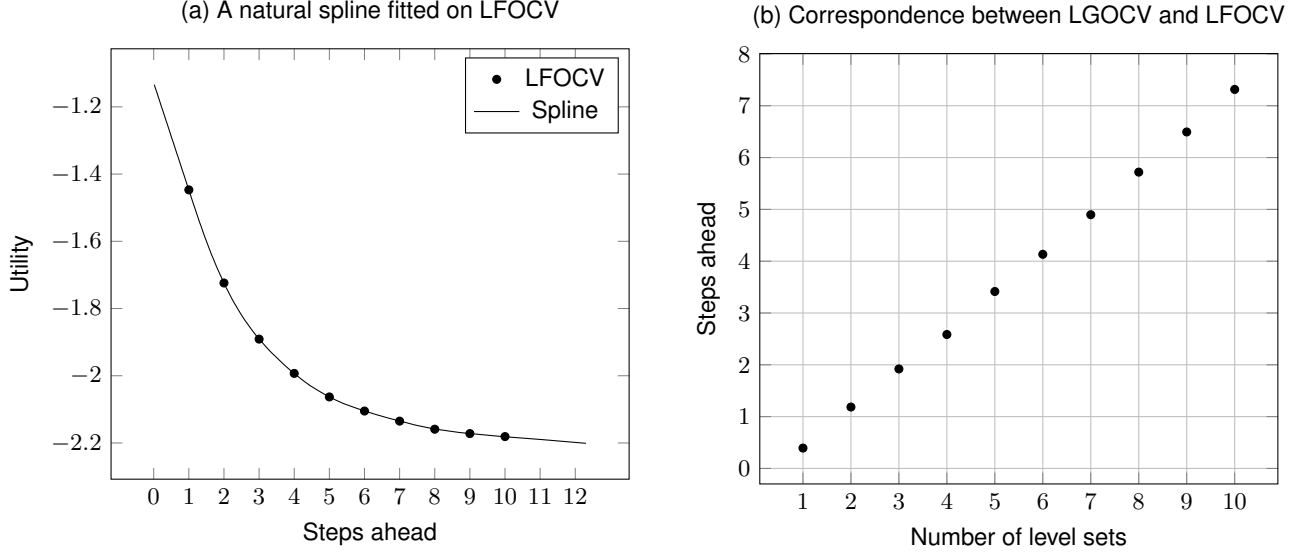


Figure 4: Automatic LGOCV compared with LFOCV

where μ is an intercept, u is a spatially structured component, v is an unstructured component [31, 34], and f_{rw} is an intrinsic second-order random-walk model of the covariate x_i [23].

In Figure 5, we display groups produced by different automatic group construction strategies. The testing point is measured from the black region, and the data in the group are measured from the grey regions. Groups in the first column are constructed by R_{prior} ; Groups in the second column are constructed by R_{prior} with only spatial effects; And groups in the third column are constructed by R_{post} . The groups constructed by R_{prior} has weak spatial pattern because the group construction also uses correlation due to tobacco consumption. The groups constructed by R_{prior} with only spatial effects have strong spatial patterns as expected. The groups constructed by R_{post} exhibit strong spatial patterns in nearly all cases, but there are also a few non-spatial patterns in the groups because it takes all the model components into consideration: the fixed and random effects, priors and the response variable. The spatial pattern in the posterior groups may provide evidence to include the spatial effects in the model since data do not destroy the spatial pattern in the correlation. In practice, the manually defined groups are more similar to the one produced by R_{prior} with selected effects. The groups produced by R_{post} are more balanced with different model components. We do not recommend using the groups produced by R_{prior} without conditioning since the covariates often affect the group construction substantially while we usually assume covariates are sampled independently.

Dengue Risk in Brazil

We will present an application of the automatic LGOCV to show the usefulness of the method in a real-world study with a complex model structure and large sample size. The variable selection process in [29] will be repeated using the automatic LGOCV with the number of level sets equal to 3. The model is aimed to quantify the non-linear and delayed effects of extreme hydrometeorological hazards on dengue risk by the level of urbanization in Brazil. The sample size of this dataset is 127, 224, which records 12, 895, 293 dengue cases. The responses in the model are monthly notified dengue cases for each of 558 microregions of Brazil between January 2001 and December 2019. The data is associated with month, year, microregion, and state. The candidate covariates in this study are the monthly mean of daily minimum temperature (T_{min}), monthly mean of daily maximum temperature (T_{max}), self-calibrated Palmer drought severity index (PDSI), level of urbanization (u), level of urbanization centered at high urbanized (u_1), level of urbanization centered at intermediate urbanized (u_2), level of urbanization centered at more rural level (u_3), access to water supply service (w), access to water supply service centered at high-frequency shortages (w_1), access to water supply service centered at intermediate shortage (w_2) and access to water supply service centered at low-frequency shortages (w_3). Information about the preprocessing of those covariates can be found in [35]. The likelihood of the model is chosen to be negative binomial to account for overdispersion. The latent field consists of a temporal component describing a state-specific seasonality using a cyclic first difference prior distribution and a spatial component describing year-specific spatially unstructured and structured random effects using a modified Besag-York-Mollie (BYM2) model with a scaled spatial component [36]. The temporal component has replications for each state and the spatial component

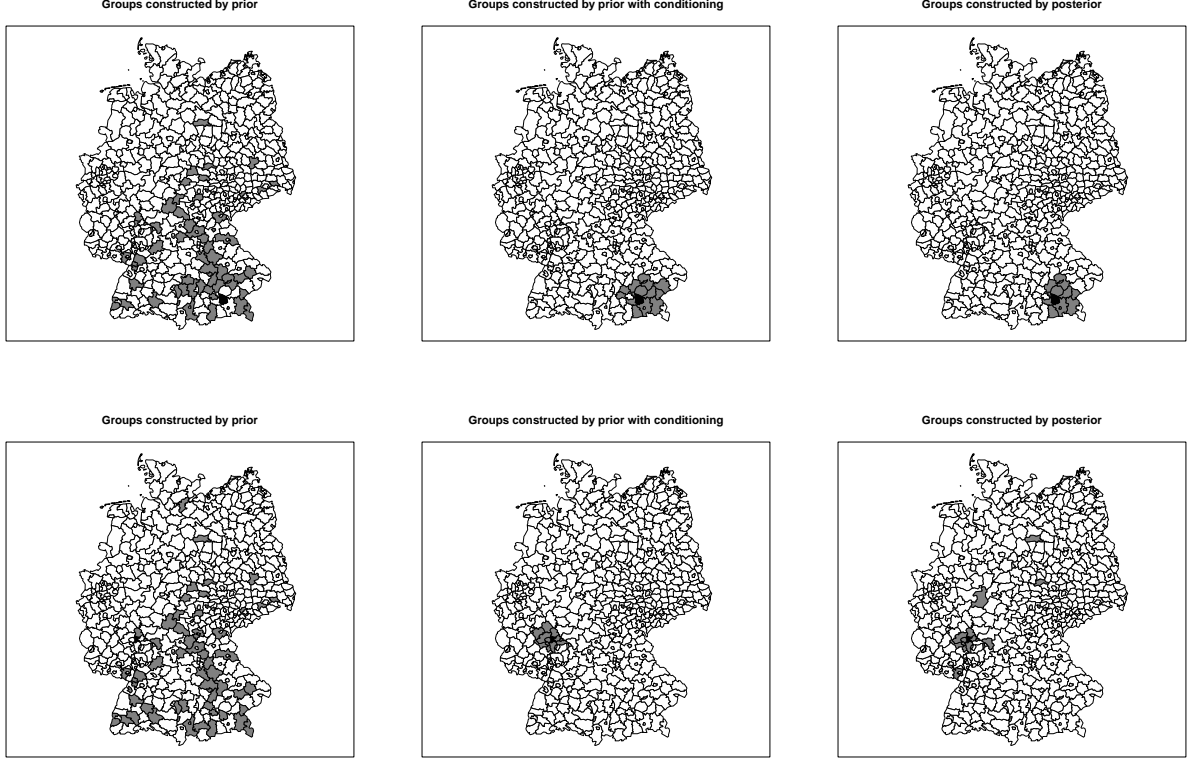


Figure 5: Groups by different automatic construction strategies

has replications for each year. We can express it using the formula,

$$\begin{aligned}
 y &\sim 1 + \text{covariates} \\
 &\quad + f(\text{month}, \text{model} = \text{"rw1"}, \text{replicates} = \text{stat}, \text{cyclic} = \text{TRUE}) \\
 &\quad + f(\text{microregion}, \text{model} = \text{"bym2"}, \text{replicates} = \text{year}).
 \end{aligned}$$

In short, we write this model as

$$y \sim 1 + \text{covariates} + f_t + f_s.$$

The number of parameters contained in this model is 21,567 for the full model. The appendix of [29] and its repository [35] provide full details about the models and data.

The model has a temporal effect with spatial replicates, a spatial effect with temporal replicates, and many constraints. It is not easy to come out with manually defined groups for LGOCV or identify important effects to include using the prior as previous examples. Thus the automatic group construction using posterior correlation is particularly useful in this rather complex model setting. Here, model 7 in Table 1 is used for groups construction.

The model selection results using DIC, LOOCV, and LGOCV are shown in Table 1. The candidate models are identical to those in [35], and the results are computed using R-INLA. The loss function is negative mean log predictive density. In the table, we find LOOCV and DIC hardly distinguish between the last 4 models while LGOCV provides more distinguishable readings. LGOCV chooses a model different from the choice of DIC and LOOCV. In conclusion, the model selected by LOOCV can be regarded as having superior predictive ability compared to those chosen based on alternative criteria.

Additionally, the group constructed by the automatic group construction using the posterior correlation matrix is interpretable. For a given testing point, the group consists of data points from the same year, the same location, and near months in most cases. Figure 6 shows the relative frequencies of the month included in the group given the testing points are records of a given month. From the graph, we may conclude that the summer data is more informative for prediction. Even when the testing point is recorded in November, the group tends to include summer data.

Index	Model	DIC	LOOCV	LGOCV
1	$y \sim 1 + f_1 + f_2$	3628	0.01502	0.03418
2	$y \sim 1 + T_{min} + f_t + f_s$	1591	0.00641	0.01217
3	$y \sim 1 + T_{max} + f_t + f_s$	2281	0.00919	0.01595
4	$y \sim 1 + PDSI + f_t + f_s$	2171	0.00921	0.02643
5	$y \sim 1 + PDSI + T_{min} + f_t + f_s$	159	0.00059	0.00510
6	$y \sim 1 + PDSI + T_{max} + f_t + f_s$	906	0.00380	0.00985
7	$y \sim 1 + PDSI + T_{min} + PDSI * u_1 + u + f_t + f_s$	44	0.00012	0.00037
8	$y \sim 1 + PDSI + T_{min} + PDSI * u_2 + u + f_t + f_s$	39	0.00012	0.00112
9	$y \sim 1 + PDSI + T_{min} + PDSI * u_3 + u + f_t + f_s$	74	0.00020	0*
10	$y \sim 1 + PDSI + T_{min} + PDSI * w_1 + w + f_t + f_s$	0*	0*	0.00460
11	$y \sim 1 + PDSI + T_{min} + PDSI * w_2 + w + f_t + f_s$	11	0.00001	0.00406
12	$y \sim 1 + PDSI + T_{min} + PDSI * w_3 + w + f_t + f_s$	10	0.00001	0.00405

Note: We offset DIC by 826858, LOOCV by 3.272018 and LGOCV by 3.524652.

Table 1: Model selection results

7 Discussion

CV is a useful tool for model assessment, but the blind trust of LOOCV is prevalent in the statistical practice, although this issue has been well-noticed [4, 37]. One reason is the lack of helpful tools to guide practitioners to design proper CV strategies and compute the corresponding CV utility. In this paper, we provide LGOCV as a framework to design proper CV and emphasize the importance of designing CV according to the prediction tasks. More importantly, we proposed an efficient approximation of the utility function and a sensible way to construct groups automatically for a large class of models. We hope these new tools for LGOCV can lead to improving statistical practice to focus more on better predictive performance measurement.

The automatic LGOCV should not be used if the modeler has a CV strategy tailored to their applications. However, having a better default CV strategy than LOOCV is a significant advantage. The automatic LGOCV is constructed by summarizing some good CV practices in structured models and our understanding of LGMs. As such, we believe that the automatic LGOCV is useful for real-world applications, and it is a good starting point to define a more suitable CV.

Acknowledgments

The authors thank D.Castro-Camilo, D.Rustand and E.Krainski for valuable discussions and suggestions.

A On the computation of $\Sigma_{\eta_{I_i}}(\theta, \mathbf{y}_{-I_i})$ and $\mu_{\eta_{I_i}}(\theta, \mathbf{y}_{-I_i})$

In this section, we let I_i be I and drop θ to simplify the notation without losing generality. We have a random vector $\eta_I | \mathbf{y} \sim N(\mu_{\eta_I}(\mathbf{y}), \Sigma_{\eta_I}(\mathbf{y}))$, which is a posterior distribution with prior $\eta_I | \mathbf{y}_{-I} \sim N(\mu_{\eta_I}(\mathbf{y}_{-I}), \Sigma_{\eta_I}(\mathbf{y}_{-I}))$ and likelihood $\pi_G(\mathbf{y}_I | \eta_I) \propto \exp \left\{ -\frac{1}{2} \eta_I^T C(\mathbf{y}_I) \eta_I + \mathbf{b}(\mathbf{y}_I) \eta_I \right\}$. Now, we need to use the posterior and the likelihood to obtain the prior.

If $\Sigma_{\eta_I}(\mathbf{y})$ is full rank, we have $\mathbf{Q}_{\eta_I}(\mathbf{y}) = \Sigma_{\eta_I}(\mathbf{y})^{-1}$ and $\mathbf{b}_{\eta_I}(\mathbf{y}) = \mathbf{Q}_{\eta_I}(\mathbf{y}) \mu_{\eta_I}(\mathbf{y})$. By conjugacy of Gaussian prior and Gaussian likelihood, $\mathbf{Q}_{\eta_I}(\mathbf{y}_{-I}) = \mathbf{Q}_{\eta_I}(\mathbf{y}) - C(\mathbf{y}_I)$ and $\mathbf{b}_{\eta_I}(\mathbf{y}_{-I}) = \mathbf{Q}_{\eta_I}(\mathbf{y}) \mu_{\eta_I}(\mathbf{y}) - \mathbf{b}(\mathbf{y}_I)$. Then we have desired $\mu_{\eta_I}(\mathbf{y}_{-I})$ and $\Sigma_{\eta_I}(\mathbf{y}_{-I})$.

If $\Sigma_{\eta_I}(\mathbf{y})$ is singular, we let $\eta | \mathbf{y} = \mathbf{B} \mathbf{z} | \mathbf{y}$, where $\mathbf{B} = \mathbf{V} \mathbf{\Lambda}$ with \mathbf{V} containing eigenvectors corresponding to non-zero eigenvalues, $\mathbf{\Lambda}$ containing square root of non-zero eigenvalues on its diagonal, and $\mathbf{z} | \mathbf{y} \sim N(\mu_{\mathbf{z}}(\mathbf{y}), \mathcal{I})$, where \mathcal{I} is an identity matrix and $\mathbf{B} \mu_{\mathbf{z}}(\mathbf{y}) = \mu_{\eta_I}(\mathbf{y})$. By conjugacy, we have $\mathbf{Q}_{\mathbf{z}}(\mathbf{y}_{-I}) = \mathcal{I} - \mathbf{B}^T C(\mathbf{y}_I) \mathbf{B}$ and $\mathbf{b}_{\mathbf{z}}(\mathbf{y}_{-I}) = \mu_{\mathbf{z}}(\mathbf{y}) - \mathbf{B}^T \mathbf{b}(\mathbf{y}_I)$. Then mean of $\mathbf{z} | \mathbf{y}_{-I}$ solves $\mathbf{Q}_{\mathbf{z}}(\mathbf{y}_{-I}) \mu_{\mathbf{z}}(\mathbf{y}_{-I}) = \mathbf{b}_{\mathbf{z}}(\mathbf{y}_{-I})$. It is followed by $\mu_{\eta_I}(\mathbf{y}_{-I}) = \mathbf{B} \mu_{\mathbf{z}}(\mathbf{y}_{-I})$ and $\Sigma_{\eta_I}(\mathbf{y}_{-I}) = \mathbf{B} \Sigma_{\mathbf{z}}(\mathbf{y}_{-I}) \mathbf{B}^T$.

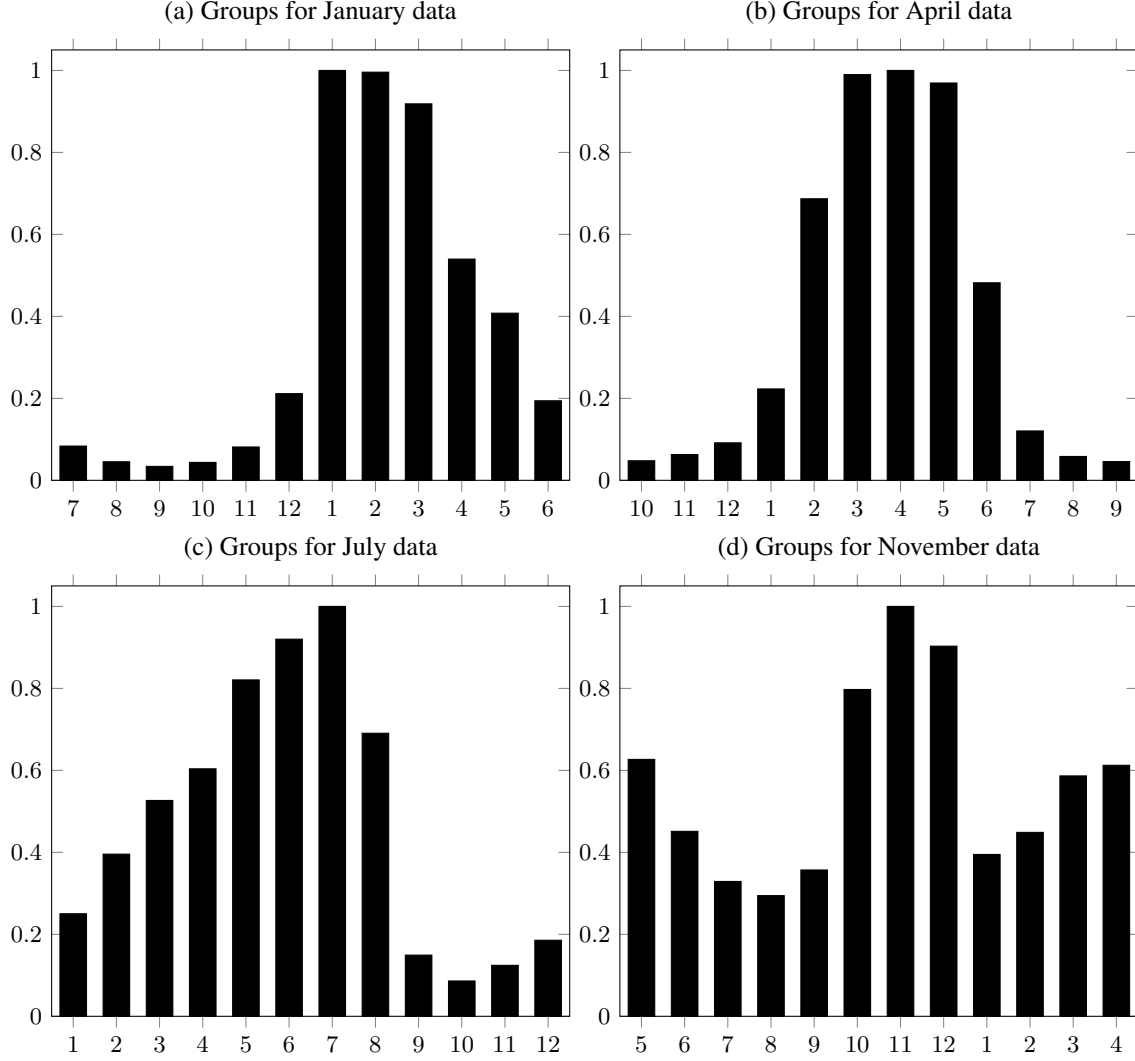


Figure 6: Groups for testing points from a given month

B On the computation of $\Sigma_{\eta_{I_i}}(\theta, y)$ and $\mu_{\eta_{I_i}}(\theta, y)$ with Linear Constraints

We start by illustrating how to compute $\Sigma_{\eta_{I_i}}(\theta, y)$ and $\mu_{\eta_{I_i}}(\theta, y)$ without linear constraints, and we apply the linear constraints to the targets. The computation of $\mu_{\eta_{I_i}}(\theta, y)$ is simple, and $\mu_{\eta_{I_i}}(\theta, y) = A_{I_i} \mu_f(\theta, y)$. However, we never store large dense matrix like $Q_f(\theta, y)^{-1}$. Thus, $\Sigma_{\eta_{I_i}}(\theta, y)$ cannot be obtained by using matrix multiplication $A_{I_i} Q_f(\theta, y)^{-1} A_{I_i}^T$. Instead, we compute $\Sigma_{\eta}(\theta, y)$ entry by entry and use the result to fill in entries of $\Sigma_{\eta_{I_i}}(\theta, y)$. We compute $\Sigma_{\eta}(\theta, y)_{i,j}$ by solving

$$Q_f(\theta, y)x = A_i$$

and $\Sigma_{\eta}(\theta, y)_{i,j} = A_j x$. The computation is fast because A and $Q_f(\theta, y)$ are sparse, and the factorization of $Q_f(\theta, y)$ is reused.

When linear constraints $\mathcal{C}f = e$ are applied on f , we have

$$\Sigma_f(\theta, y)^* = Q_f(\theta, y)^{-1} - Q_f(\theta, y)^{-1} \mathcal{C}^T (\mathcal{C} Q_f(\theta, y)^{-1} \mathcal{C}^T)^{-1} \mathcal{C} Q_f(\theta, y)^{-1},$$

$$\mu_f(\theta, y)^* = \mu_f(\theta, y) - Q_f(\theta, y)^{-1} \mathcal{C}^T (\mathcal{C} Q_f(\theta, y)^{-1} \mathcal{C}^T)^{-1} (\mathcal{C} \mu_f - e),$$

where $\Sigma_f(\theta, y)^*$ and $\mu_f(\theta, y)^*$ are the mean and the covariance matrix after applying constraints [23]. Because $\mu_f(\theta, y)^*$ is always stored, the computation of $\mu_{\eta_{I_i}}(\theta, y)$ is simple. We need to propagate the effects of linear

constraints to $\Sigma_{\eta}(\theta, \mathbf{y})_{i,j}$. This is achieved by computing [23]

$$\mathbf{x}^* = \mathbf{x} - \mathbf{Q}_f(\theta, \mathbf{y})^{-1} \mathbf{C}^T (\mathbf{C} \mathbf{Q}_f(\theta, \mathbf{y})^{-1} \mathbf{C}^T)^{-1} \mathbf{C} \mathbf{x},$$

where \mathbf{x} solves $\mathbf{Q}_f(\theta, \mathbf{y}) \mathbf{x} = \mathbf{A}_i$. Then

$$\Sigma_{\eta}(\theta, \mathbf{y})_{i,j}^* = \mathbf{A}_j \mathbf{x}^*,$$

where $\Sigma_{\eta}(\theta, \mathbf{y})_{i,j}^*$ is the result of propagating the effects of linear constraints to $\Sigma_{\eta}(\theta, \mathbf{y})_{i,j}$.

References

- [1] Trevor Hastie, Robert Tibshirani, Jerome H Friedman, and Jerome H Friedman. *The elements of statistical learning: data mining, inference, and prediction*, volume 2. Springer, 2009.
- [2] Andrew Gelman, John B Carlin, Hal S Stern, and Donald B Rubin. *Bayesian data analysis*. Chapman and Hall/CRC, 1995.
- [3] Assaf Rabinowicz and Saharon Rosset. Cross-validation for correlated data. *Journal of the American Statistical Association*, pages 1–14, 2020.
- [4] David R Roberts, Volker Bahn, Simone Ciuti, Mark S Boyce, Jane Elith, Gurutzeta Guillera-Aroita, Severin Hauenstein, José J Lahoz-Monfort, Boris Schröder, Wilfried Thuiller, et al. Cross-validation strategies for data with temporal, spatial, hierarchical, or phylogenetic structure. *Ecography*, 40(8):913–929, 2017.
- [5] Sohrab Saeb, Luca Lonini, Arun Jayaraman, David C Mohr, and Konrad P Kording. The need to approximate the use-case in clinical machine learning. *Gigascience*, 6(5):gix019, 2017.
- [6] Leopoldo M Ruiz Maraggi, Larry W Lake, and Mark P Walsh. Using bayesian leave-one-out and leave-future-out cross-validation to evaluate the performance of rate-time models to forecast production of tight-oil wells. In *SPE/AAPG/SEG Unconventional Resources Technology Conference*. OnePetro, 2021.
- [7] Paul-Christian Bürkner, Jonah Gabry, and Aki Vehtari. Approximate leave-future-out cross-validation for bayesian time series models. *Journal of Statistical Computation and Simulation*, 90(14):2499–2523, 2020.
- [8] RJ Telford and HJB Birks. Evaluation of transfer functions in spatially structured environments. *Quaternary Science Reviews*, 28(13-14):1309–1316, 2009.
- [9] Prabir Burman, Edmond Chow, and Deborah Nolan. A cross-validatory method for dependent data. *Biometrika*, 81(2):351–358, 1994.
- [10] Arthur P Dempster, Nan M Laird, and Donald B Rubin. Maximum likelihood from incomplete data via the em algorithm. *Journal of the Royal Statistical Society: Series B (Methodological)*, 39(1):1–22, 1977.
- [11] Rebecca R Andridge and Roderick JA Little. A review of hot deck imputation for survey non-response. *International statistical review*, 78(1):40–64, 2010.
- [12] Michael L Stein. *Interpolation of spatial data: some theory for kriging*. Springer Science & Business Media, 2012.
- [13] Håvard Rue, Sara Martino, and Nicolas Chopin. Approximate bayesian inference for latent gaussian models by using integrated nested laplace approximations. *Journal of the royal statistical society: Series b (statistical methodology)*, 71(2):319–392, 2009.
- [14] Janet Van Niekerk, Elias Krainski, Denis Rustand, and Haavard Rue. A new avenue for bayesian inference with inla. *arXiv preprint arXiv:2204.06797*, 2022.
- [15] Aki Vehtari, Andrew Gelman, and Jonah Gabry. Practical bayesian model evaluation using leave-one-out cross-validation and waic. *Statistics and computing*, 27(5):1413–1432, 2017.
- [16] Olivier Dubrule. Cross validation of kriging in a unique neighborhood. *Journal of the International Association for Mathematical Geology*, 15(6):687–699, 1983.
- [17] David Ginsbourger and Cedric Schärer. Fast calculation of gaussian process multiple-fold cross-validation residuals and their covariances. *arXiv preprint arXiv:2101.03108*, 2021.
- [18] Soumya Ghosh, William T Stephenson, Tin D Nguyen, Sameer K Deshpande, and Tamara Broderick. Approximate cross-validation for structured models. *arXiv preprint arXiv:2006.12669*, 2020.
- [19] Tilmann Gneiting and Adrian E Raftery. Strictly proper scoring rules, prediction, and estimation. *Journal of the American statistical Association*, 102(477):359–378, 2007.

- [20] Daniel Commenges, Benoit Lique, and Cécile Proust-Lima. Choice of prognostic estimators in joint models by estimating differences of expected conditional kullback–leibler risks. *Biometrics*, 68(2):380–387, 2012.
- [21] Håvard Rue, Andrea Riebler, Sigrunn H Sørbye, Janine B Illian, Daniel P Simpson, and Finn K Lindgren. Bayesian computing with inla: a review. *Annual Review of Statistics and Its Application*, 4:395–421, 2017.
- [22] Janet van Niekerk and Haavard Rue. Correcting the laplace method with variational bayes. *arXiv preprint arXiv:2111.12945*, 2021.
- [23] Havard Rue and Leonhard Held. *Gaussian Markov random fields: theory and applications*. Chapman and Hall/CRC, 2005.
- [24] Sumio Watanabe and Manfred Opper. Asymptotic equivalence of bayes cross validation and widely applicable information criterion in singular learning theory. *Journal of machine learning research*, 11(12), 2010.
- [25] Sumio Watanabe. Information criteria and cross validation for bayesian inference in regular and singular cases. *Japanese Journal of Statistics and Data Science*, 4(1):1–19, 2021.
- [26] Aki Vehtari, Janne Ojanen, et al. A survey of bayesian predictive methods for model assessment, selection and comparison. *Statistics Surveys*, 6:142–228, 2012.
- [27] Qing Liu and Donald A Pierce. A note on gauss—hermite quadrature. *Biometrika*, 81(3):624–629, 1994.
- [28] Andrew M Walker. On the asymptotic behaviour of posterior distributions. *Journal of the Royal Statistical Society: Series B (Methodological)*, 31(1):80–88, 1969.
- [29] Rachel Lowe, Sophie A Lee, Kathleen M O’Reilly, Oliver J Brady, Leonardo Bastos, Gabriel Carrasco-Escobar, Rafael de Castro Catão, Felipe J Colón-González, Christovam Barcellos, Marília Sá Carvalho, et al. Combined effects of hydrometeorological hazards and urbanisation on dengue risk in brazil: a spatiotemporal modelling study. *The Lancet Planetary Health*, 5(4):e209–e219, 2021.
- [30] Stan Development Team. RStan: the R interface to Stan, 2022. R package version 2.21.5.
- [31] Julian Besag, Jeremy York, and Annie Mollié. Bayesian image restoration, with two applications in spatial statistics. *Annals of the institute of statistical mathematics*, 43(1):1–20, 1991.
- [32] Jonathan C Wakefield, NG Best, and L Waller. Bayesian approaches to disease mapping. *Spatial epidemiology: methods and applications*, pages 104–127, 2000.
- [33] Leonhard Held, Isabel Natário, Sarah Elaine Fenton, Håvard Rue, and Nikolaus Becker. Towards joint disease mapping. *Statistical methods in medical research*, 14(1):61–82, 2005.
- [34] Annie Mollié. Bayesian mapping of disease. *Markov chain Monte Carlo in practice*, 1:359–379, 1996.
- [35] Rachel Lowe. Data and R code to accompany ‘Combined effects of hydrometeorological hazards and urbanisation on dengue risk in Brazil: a spatiotemporal modelling study’, March 2021.
- [36] Andrea Riebler, Sigrunn H Sørbye, Daniel Simpson, and Håvard Rue. An intuitive bayesian spatial model for disease mapping that accounts for scaling. *Statistical methods in medical research*, 25(4):1145–1165, 2016.
- [37] Aki Vehtari, Daniel P Simpson, Yuling Yao, and Andrew Gelman. Limitations of “limitations of bayesian leave-one-out cross-validation for model selection”. *Computational Brain & Behavior*, 2(1):22–27, 2019.